Choroidal and Retinal Thicknesses in Healthy Eyes Measured with Ultra-Wide Field Optical Coherence Tomography

Krzysztof Kiciński and Maciej Gawęcki *

Article

Choroidal and Retinal Thicknesses in Healthy Eyes Measured with Ultra-Wide Field Optical Coherence Tomography

Krzysztof Kiciński [1] **and Maciej Gawęcki** [1,2,*]

[1] Department of Ophthalmology of Pomeranian Hospitals, 84-120 Wejherowo, Poland
[2] Dobry Wzrok Ophthalmological Clinic, 80-822 Gdansk, Poland
* Correspondence: maciej@gawecki.com; Tel.: +0048 501788654

Abstract: Ultra-wide field optical coherence tomography (UWF-OCT) has been recently introduced into clinical ophthalmological practice. To date, there is little data on the reference values of retinal thickness (RT) and choroidal thickness (CT) measured with this technique. This study aimed to analyze the variance of RT and CT in healthy eyes with UWF-OCT tests performed with the largest available scan size of 23 x 20 mm. The data were analyzed with reference to the patients' age, gender, and the axial length of the eyeball. The results of UWF-OCT scanning enabled us to picture the shape of the retina and choroid in a large portion of the eyeball. Both anatomical entities become significantly thinner at the periphery. The peripheral CT is greater in the upper and temporal sectors; the RT is higher in the nasal compared to the temporal sectors. Both choroid and retina lose thickness with age, however, CT and RT do not show a statistically significant correlation with the axial length after adjusting for age and gender. Age-related variations in thickness are especially prominent in the choroid. The CT in UWF-OCT testing is significantly greater in females while the RT is greater in males. UWF-OCT testing provides additional information on the anatomical structure of the retina and choroid compared to standard-field OCT.

Keywords: ultra-wide field optical coherence tomography; choroidal thickness; retinal thickness; axial length

1. Introduction

Determining normative databases in chorioretinal diseases is important for the precise evaluation of ocular pathologies. This is especially valid for optical coherence tomography (OCT) devices that provide measurements of the retina and the choroid [1,2]. So far, the most popular databases refer to the central retinal thickness (RT) measured within the Early Treatment Diabetic Retinopathy Study (ETDRS) grid and the retinal nerve fiber layer (RNFL) thickness assessed in glaucoma [3,4]. The choroidal thickness (CT) database is not yet available in most OCT devices, partly due to its major variance depending on the patient's age and the axial length of the eyeball [5]. Nevertheless, up-to-date research provides some data on CT in healthy individuals, usually limited to the central area of the posterior pole [6]. This is because wide-field (WF) OCT devices have just been introduced into clinical practice and are not yet commonly used in ophthalmological clinics. As peripheral retinal changes often correlate with central ocular pathologies, determining the reference thickness values for the peripheral retina and choroid would enable a more precise evaluation of ocular disorders in general [7–9].

The goal of our study was to analyze the variance of RT and CT in healthy eyes with WF-OCT testing performed with the largest available scan size of 23 x 20 mm. The data were analyzed with reference to the patients' age, gender, and the axial length of the eyeball.

2. Materials and Methods

The study included 75 consecutive patients admitted to the outpatient ophthalmological clinic at the Specialist Hospital in Chojnice, Poland, between May and June 2023 for a routine ophthalmological check-up including the prescription of spectacles. All patients underwent a routine ophthalmological examination that included best-corrected visual acuity testing, automated refraction, biomicroscopy of the anterior and posterior segments of the eye and intraocular pressure measurement. The eyes without ocular pathologies or previous ocular surgical treatment were initially qualified for wide-field OCT testing. Cases with refraction error larger than 6.0 D in myopia, 4D in hypermetropia, and 3 D in astigmatism were excluded. Patients burdened with systemic diseases that could influence the results, especially diabetes mellitus, hypertension, hypercholesterolemia, metabolic disorders or pregnancy were also excluded from the study group. Implementation of these criteria resulted in exclusion of 80 patients and 25 fellow eyes, thus altogether 125 eyes were included in the study. The baseline characteristics of the cohort are presented in Table I.

Table 1. Baseline characteristics of the control group (discrete variables, n = 75 individuals).

Analyzed trait	No and (percentage in %.)
No. of participants	75 (50,68)
No. of eyes	125 (43,60)
Gender:	
- **Female**	48 (64,00)
- **Male**	27 (36,00)
Age group (years):	
- **Up to 40**	24 (19,20)
- **41–50**	12 (9,60)
- **51–60**	33 (26,40)
- **61–70**	20 (16,00)
- **Over 70**	36 (28,80)

Before the examination all patients were asked to restrain from consuming coffee or smoking. All scans were obtained at the same time of the day in the morning to exclude the impact of diurnal variability of RT and CT. Measurements were performed after pupil dilation with a swept-source Xephilio OCT-S1 (Canon Medical Systems Europe B.V. , 2023). The device provides scanning speed at 100000 A scan per second, horizontal resolution of 30μm, axial resolution of 8μm and the range of scan width from 3 – 23 mm. The protocol that was used enabled to capture a retinal area of 23 x 20 mm with measurements performed in 25 sectors enclosed in a circle of 18 mm in diameter. The sector arrangement is provided in the Xephilio device. The segmentation of layers was manually checked and corrected if necessary. The results for neighboring fields were added to represent larger retinal areas. Altogether, nine fields were analyzed: central, superonasal (SN), superotemporal (ST), inferotemporal (IT), inferonasal (IN), peripheral superonasal (SNp), peripheral superotemporal (STp), peripheral inferotemporal (ITp), and peripheral inferonasal (INp). The central area refers to the central circle of 3 mm in diameter; the SN, ST, IT, and IN areas are localized between the central 3 mm circle and the larger 9 mm circle; the SNp, STp, ITp, and INp areas are located between the 9 mm circle and the 18 mm circle. The dimensions and shapes of the analyzed retinal areas are shown in Figure 1. The obtained measurement data represent average thickness values in each of the fields. Only the scans suitable for numeric evaluation were included in the analysis. Additional data obtained from the standard measurement protocol included the axial length of the eyeball in mm.
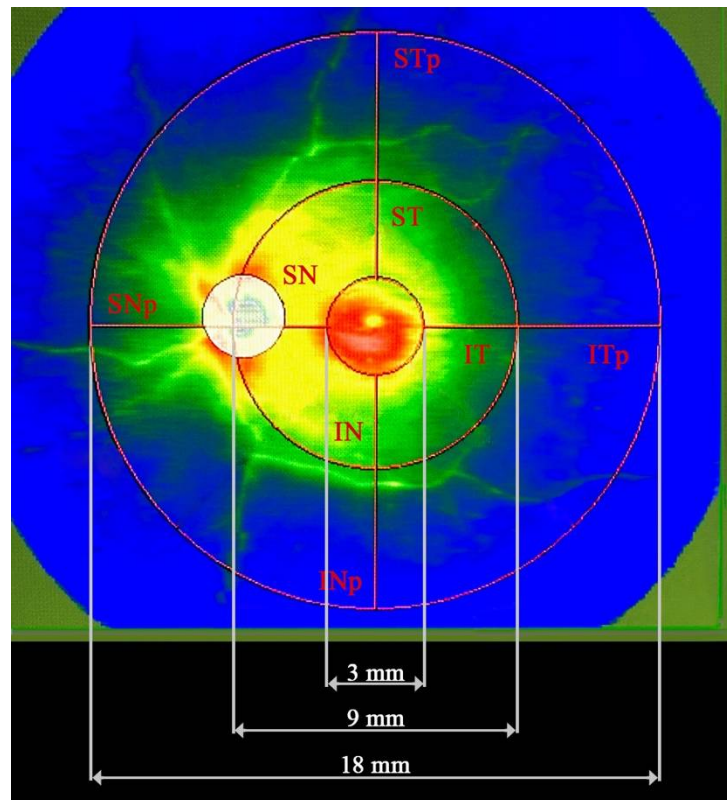
Figure 1. Visualization of the nine fields included in the analysis. SN: superonasal, ST: superotemporal, IT: inferotemporal, IN: inferonasal, SNp: peripheral superonasal, STp: peripheral superotemporal, ITp: peripheral inferotemporal, INp: peripheral inferonasal.

2.1. Statistical Procedures

Categorical traits were described through integer numbers and percentages. Numerical traits were depicted by using their mean, median, standard deviation, and lower-to-upper quartile values. The normality of the distribution was assessed using the Shapiro–Wilk W-test. Levene's test was used to assess the homogeneity of variances. A multifactor analysis of variance (ANOVA) was performed to test the significance of differences in normally distributed numerical traits between the study groups. When dealing with non-normally distributed quantitative variables, generalized linear models were used. The Pearson product-moment correlation coefficient r was computed when assessing the relationships between selected numerical traits. All the procedures were performed by using Statistica™ release 13 (TIBCO Software Inc., Palo Alto, CA, USA).

3. Results

Analysis of the RT and CT across sectors revealed significant variance between all sectors at $p < 0.0001$ (Tables II and III). Significant differences were also found in pairwise comparisons in each pair of measured retinal areas and all but two comparisons in choroidal areas (Tables IV and V). As expected, the retina and choroid are thickest in the central region. As we move to the periphery, the retinal and choroidal thicknesses are significantly lower (Table II). Temporal sectors have higher CT values compared to nasal sectors; superior quadrants have greater thickness values than inferior quadrants. Conversely, RT is higher in nasal sectors compared to temporal ones. A greater CT in the central 3 mm area correlated positively with the retinal thickness in that region ($r = 0{,}21$; $p = 0{,}0116$).

In general, male patients had thicker retinas than female patients. This difference was significant for the central and paracentral portions of the retina but not the far peripheral, where thickness values were similar in both genders. Conversely, females had greater choroidal thickness than males. Although the difference was not significant in the central area of 3 mm diameter, it was very apparent in all other sectors, including the far periphery (Table VI).

Analysis of the retinal and choroidal thicknesses by age provided straightforward results for the central and paracentral sectors. The sectoral retinal and choroidal thicknesses in these areas diminish

with age. Such variation is especially prominent in the choroid. The difference between the central CT in patients younger than 40 and those in their 80s is approximately 100 μm, which is almost 30% of the baseline value. For the retina, such correlation is also significant but less apparent numerically. It seems that significant retinal thinning (total and sectoral) occurs late, that is, in the 8th decade of life. A clear difference in RT was observed between patients over 70 and those under 40, although it did not exceed 14 μm (4% of the baseline value) in any of the measured sectors. Moreover, the retinal areas located at the far periphery did not show strong thickness variation with age. Examples of difference in CT and RT between young and older individuals are presented in Figure 2 and Figure 3.

The mean axial length value was 24.79 +/- 1.60 mm and generally did not correlate with RT or CT after adjusting for age and gender (Table VIII).

Table 2. Descriptive statistics for the parafoveal retinal thickness (μm) in the control group (n = 125 eyes).

Retinal thickness (μm)	Statistical parameter				p-value *
	M	*SD*	*Me*	*Q₁–Q₃*	
Central	335,08	20,69	335,00	324,00–348,00	
ST	271,90	14,10	273,75	262,00–282,00	
SN	309,65	16,69	311,50	299,00–320,25	
IN	300,99	17,91	302,50	289,25–311,50	
IT	267,42	16,51	268,75	259,00–278,00	**< 0,0001**
STp	212,32	10,60	212,00	205,00–220,00	
SNp	242,94	16,29	243,50	232,00–254,50	
INp	220,38	15,42	219,50	210,00–230,00	
ITp	205,52	11,69	206,00	199,00–214,00	

(* Controlled for the study subjects' gender.). SN: superonasal, ST: superotemporal, IT: inferotemporal, IN: inferonasal, SNp: peripheral superonasal, STp: peripheral superotemporal, ITp: peripheral inferotemporal, INp: peripheral inferonasal, M: mean, Me: median, SD: standard deviation, Q: quartile.

Table 3. Descriptive statistics for the parafoveal choroidal thickness (μm) in the control group (n = 125 eyes).

Choroidal thickness (μm)	Statistical parameter				p-value *
	M	*SD*	*Me*	*Q₁–Q₃*	
Central	293,90	87,10	300,00	223,00–357,00	
ST	283,94	77,20	285,00	223,25–348,00	
SN	244,60	75,52	245,25	184,00–307,75	
IN	218,72	75,10	204,25	162,75–289,25	
IT	256,65	79,29	246,00	192,00–312,75	**< 0,0001**
STp	225,16	54,80	219,00	183,50–261,50	
SNp	192,38	57,77	189,00	151,50–237,50	
INp	139,98	39,78	129,50	107,50–163,00	
ITp	188,75	48,50	179,00	150,00–226,00	

(* Controlled for the study subjects' age and gender.). SN: superonasal, ST: superotemporal, IT: inferotemporal, IN: inferonasal, SNp: peripheral superonasal, STp: peripheral superotemporal, ITp: peripheral inferotemporal, INp: peripheral inferonasal, M: mean, Me: median, SD: standard deviation, Q: quartile.

Table 4. Comparisons between retinal thickness measurements.

RT	Central	ST	SN	IN	IT	STp	SNp	INp
ST	< 0,0001							
SN	< 0,0001	< 0,0001						
IN	< 0,0001	< 0,0001	< 0,0001					

IT	< 0,0001	< 0,0001	< 0,0001	< 0,0001				
STp	< 0,0001	< 0,0001	< 0,0001	< 0,0001	< 0,0001			
SNp	< 0,0001	< 0,0001	< 0,0001	< 0,0001	< 0,0001	< 0,0001		
INp	< 0,0001	< 0,0001	< 0,0001	< 0,0001	< 0,0001	< 0,0001	< 0,0001	
ITp	< 0,0001	< 0,0001	< 0,0001	< 0,0001	< 0,0001	< 0,0001	< 0,0001	< 0,0001

RT: retinal thickness, SN: superonasal, ST: superotemporal, IT: inferotemporal, IN: inferonasal, SNp: peripheral superonasal, STp: peripheral superotemporal, ITp: peripheral inferotemporal, INp: peripheral inferonasal.

Table 5. Comparisons between choroidal thickness measurements.

CT	Central	ST	SN	IN	IT	STp	SNp	INp
ST	= 0,0148							
SN	< 0,0001	< 0,0001						
IN	< 0,0001	< 0,0001	< 0,0001					
IT	< 0,0001	< 0,0001	< 0,0001	< 0,0001				
STp	< 0,0001	< 0,0001	< 0,0001	= 0,1744	< 0,0001			
SNp	< 0,0001	< 0,0001	< 0,0001	< 0,0001	< 0,0001	< 0,0001		
INp	< 0,0001	< 0,0001	< 0,0001	< 0,0001	< 0,0001	< 0,0001	< 0,0001	
ITp	< 0,0001	< 0,0001	< 0,0001	< 0,0001	< 0,0001	< 0,0001	= 0,2615	< 0,0001

CT: choroidal thickness, SN: superonasal, ST: superotemporal, IT: inferotemporal, IN: inferonasal, SNp: peripheral superonasal, STp: peripheral superotemporal, ITp: peripheral inferotemporal, INp: peripheral inferonasal.

Table 6. Retinal and choroidal thicknesses in the control group by gender (numerical variables, n = 125 eyes).

Analyzed trait	Gender	Statistical parameter *				p-value **
		M	*SD*	*Me*	Q_1–Q_3	
Central RT (μm)	**Male**	340,43	23,86	342,50	332,00–360,00	**= 0,0191**
	Female	332,17	18,26	334,00	323,00–345,00	
ST	**Male**	274,93	14,61	276,62	262,12–283,88	**= 0,0007**
	Female	270,26	13,62	272,25	262,00–278,50	
SN	**Male**	312,35	17,05	313,87	301,87–324,63	**= 0,0013**
	Female	308,18	16,41	311,00	297,75–319,75	
IN	**Male**	306,52	16,79	305,62	296,62–317,75	**= 0,0148**
	Female	297,98	17,87	299,00	287,75–310,25	
IT	**Male**	271,19	16,67	273,25	260,37–280,38	**= 0,0145**
	Female	265,44	16,17	267,00	258,75–275,00	
STp	**Male**	216,30	10,23	217,00	208,00–223,75	= 0,1218
	Female	210,17	10,23	210,00	203,50–215,50	
SNp	**Male**	249,59	15,53	250,25	238,00–259,75	**= 0,0241**
	Female	239,32	15,63	238,50	228,00–247,50	
INp	**Male**	227,05	12,61	227,25	217,75–232,25	= 0,5537
	Female	216,75	15,66	216,00	205,50–227,50	
ITp	**Male**	209,75	10,18	211,50	201,25–217,00	= 0,3419
	Female	203,23	11,87	203,00	197,00–212,00	
Central CT (μm)	**Male**	284,70	79,44	289,00	218,00–343,50	= 0,5435
	Female	298,89	91,08	300,00	227,00–359,00	
ST	**Male**	263,13	68,92	265,87	208,50–318,38	**< 0,0001**
	Female	295,25	79,48	301,50	237,25–359,50	
SN	**Male**	239,19	73,25	232,75	175,12–293,38	**= 0,0009**
	Female	247,53	77,02	247,25	197,50–309,75	
IN	**Male**	218,36	66,08	213,87	161,12–281,13	**= 0,0005**
	Female	218,91	79,98	200,50	162,75–291,25	
IT	**Male**	239,76	65,72	240,75	186,12–281,88	**< 0,0001**
	Female	265,82	84,74	251,75	195,25–336,50	

STp	Male	211,97	44,98	209,50	180,75–248,25	< 0,0001
	Female	232,33	58,48	232,00	184,50–269,50	
SNp	Male	179,68	44,73	171,50	145,50–202,00	= 0,0106
	Female	199,28	62,94	195,00	151,50–243,00	
INp	Male	133,90	27,82	127,75	112,50–151,00	= 0,0131
	Female	143,28	44,79	130,00	107,00–175,50	
ITp	Male	175,33	41,51	159,75	144,50–217,75	< 0,0001
	Female	196,04	50,67	185,00	155,50–230,50	

(* Statistical parameters used: M: mean, SD: standard deviation, Me: median, Q: quartiles. ** Controlled for the study subjects' age.). RT: retinal thickness, CT: choroidal thickness, SN: superonasal, ST: superotemporal, IT: inferotemporal, IN: inferonasal, SNp: peripheral superonasal, STp: peripheral superotemporal, ITp: peripheral inferotemporal, INp: peripheral inferonasal.

Table 7. Retinal and choroidal thicknesses in the control group by age (numerical variables, n = 125 eyes).

Analyzed trait	Age group (years)	Statistical parameter *				p-value **
		M	SD	Me	Q_1–Q_3	
Central RT (μm)	Up to 40	336,55	15,16	340,50	324,25–348,58	= 0,0388
	41–50	337,58	12,00	342,50	326,42–247,58	
	51–60	344,00	17,88	344,50	336,08–353,58	
	61–70	338,30	25,51	334,00	328,00–352,67	
	Over 70	326,67	21,97	330,50	311,42–338,17	
ST	Up to 40	276,91	18,78	279,62	276,46–283,79	= 0,0017
	41–50	275,44	10,82	277,12	268,60–284,44	
	51–60	278,27	6,82	277,75	272,35–283,17	
	61–70	271,39	13,18	267,75	260,83–280,58	
	Over 70	265,12	13,34	263,12	256,85–272,42	
SN	Up to 40	315,90	19,36	320,00	303,48–328,65	= 0,0041
	41–50	314,85	14,70	315,50	308,87–321,88	
	51–60	314,96	9,75	315,12	306,29–319,75	
	61–70	307,53	15,16	308,25	298,25–317,08	
	Over 70	302,87	17,29	301,00	291,56–318,00	
IN	Up to 40	304,12	23,71	312,12	288,60–321,83	= 0,0072
	41–50	306,54	13,08	309,62	303,92–315,44	
	51–60	307,06	11,99	304,12	297,31–315,21	
	61–70	301,45	17,19	299,50	291,67–310,33	
	Over 70	293,10	17,31	294,00	282,25–307,42	
IT	Up to 40	270,44	22,21	274,62	269,67–282,31	= 0,0129
	41–50	271,71	11,37	272,87	262,35–279,46	
	51–60	272,56	7,98	270,37	267,00–278,85	
	61–70	269,33	15,00	267,00	258,67–279,25	
	Over 70	259,56	17,13	260,25	249,31–268,33	
STp	Up to 40	213,00	11,78	212,00	209,92–220,25	= 0,1967
	41–50	213,73	9,33	210,75	206,42–222,17	
	51–60	214,00	7,48	214,50	206,92–220,79	
	61–70	214,15	11,27	214,50	205,00–220,67	
	Over 70	208,78	10,64	208,25	200,00–216,38	
SNp	Up to 40	244,43	18,35	245,00	236,63–250,96	= 0,0141
	41–50	243,81	14,66	244,50	233,13–257,83	
	51–60	247,29	12,61	250,50	236,13–255,67	
	61–70	248,82	18,22	251,00	232,50–259,67	
	Over 70	234,68	12,33	233,50	228,00–241,79	
INp	Up to 40	220,88	18,49	224,00	210,45–231,29	= 0,3508

	41–50	218,46	11,94	218,75	210,00–228,29	
	51–60	220,21	9,37	221,00	212,46–228,75	
	61–70	226,53	17,96	227,50	212,17–238,67	
	Over 70	215,79	13,45	215,75	206,42–225,75	
ITp	Up to 40	206,23	16,14	206,50	200,71–216,67	= 0,3770
	41–50	206,75	9,39	204,75	200,21–212,29	
	51–60	205,67	6,50	205,75	199,75–210,38	
	61–70	208,11	11,17	209,50	199,33–217,00	
	Over 70	201,90	11,68	202,25	194,71–213,29	
Central CT (μm)	Up to 40	345,20	84,63	348,50	309,17–395,50	< 0,0001
	41–50	329,00	68,41	321,50	289,17–373,25	
	51–60	288,50	111,02	259,00	196,75–394,42	
	61–70	286,33	66,65	281,00	260,00–338,33	
	Over 70	250,72	87,46	229,50	181,75–325,83	
ST	Up to 40	339,04	70,66	345,37	297,31–380,81	= 0,0002
	41–50	311,45	73,91	306,50	254,85–388,38	
	51–60	278,58	80,97	262,75	196,27–359,00	
	61–70	269,54	53,54	266,25	235,25–314,33	
	Over 70	249,98	80,54	238,37	190,44–310,13	
SN	Up to 40	274,55	74,53	293,37	226,90–340,08	= 0,0809
	41–50	260,87	63,83	239,12	212,60–321,88	
	51–60	251,52	84,97	246,37	175,87–329,33	
	61–70	241,94	65,57	247,50	206,00–274,67	
	Over 70	217,24	82,63	204,62	144,60–286,25	
IN	Up to 40	252,46	63,59	270,00	218,17–299,73	= 0,0217
	41–50	239,48	69,80	211,75	174,79–309,83	
	51–60	223,12	89,06	194,12	146,98–284,35	
	61–70	212,36	92,93	204,50	183,67–263,50	
	Over 70	190,48	81,63	160,75	128,77–227,73	
IT	Up to 40	299,30	72,50	292,62	257,08–342,94	= 0,0021
	41–50	289,04	77,39	272,75	222,00–355,63	
	51–60	258,87	107,23	218,50	182,62–653,60	
	61–70	242,96	62,02	240,25	201,67–274,67	
	Over 70	223,15	72,54	193,87	155,35–257,23	
STp	Up to 40	274,23	40,18	259,25	240,08–313,71	< 0,0001
	41–50	240,98	54,80	237,75	199,42–271,88	
	51–60	224,79	46,28	234,75	180,12–267,21	
	61–70	209,86	36,25	210,50	196,00–222,50	
	Over 70	201,50	59,76	190,75	154,24–242,13	
SNp	Up to 40	217,75	53,90	234,50	176,58–256,21	= 0,2324
	41–50	200,06	52,46	186,00	159,00–256,42	
	51–60	199,96	70,33	162,00	141,37–243,67	
	61–70	179,82	38,77	174,50	157,83–198,17	
	Over 70	183,17	69,71	168,00	129,50–211,29	
INp	Up to 40	161,10	36,41	161,25	134,79–191,08	= 0,1168
	41–50	142,52	38,28	129,00	109,67–165,04	
	51–60	141,88	38,64	128,00	109,5–172,83	
	61–70	131,64	24,76	130,00	116,50–148,00	
	Over 70	133,57	50,27	111,00	98,71–150,25	
ITp	Up to 40	219,10	31,22	224,00	196,46–237,92	= 0,0029
	41–50	202,63	49,94	182,25	163,42–248,67	
	51–60	195,83	62,17	167,00	149,96–242,67	
	61–70	177,62	39,24	170,50	151,67–198,83	
	Over 70	170,40	49,09	152,50	133,67–194,97	

(* Statistical parameters used: M: mean, SD: standard deviation, Me: median, Q: quartiles. ** Controlled for the study subjects' age and gender.). RT: retinal thickness, CT: choroidal thickness, SN: superonasal, ST: superotemporal, IT: inferotemporal, IN: inferonasal, SNp: peripheral superonasal, STp: peripheral superotemporal, ITp: peripheral inferotemporal, INp: peripheral inferonasal.
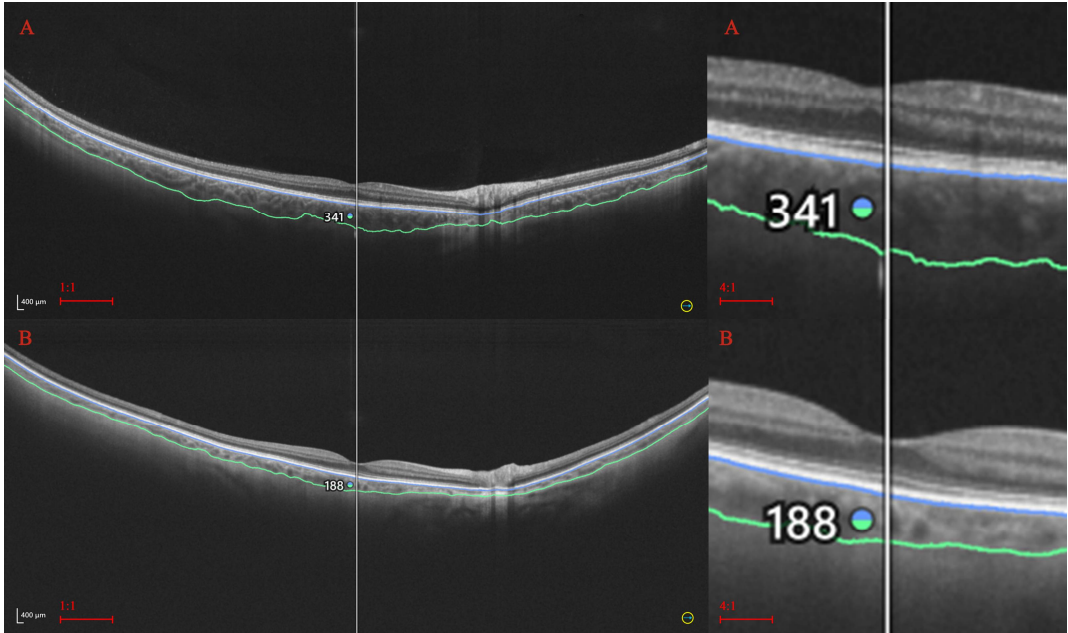
Table 8. Pearson product-moment correlation coefficients and corresponding *p* values for the axial length *versus* the retinal thickness and choroidal thickness in the control group.

Thickness (µm)	Axial length (mm)	
	r	*p* *
Central RT	−0,09	0,3496
ST	−0,14	0,1523
SN	−0,15	0,1042
IN	**−0,19**	**0,0491**
IT	−0,14	0,1408
STp	−0,05	0,6152
SNp	−0,13	0,1729
INp	0,05	0,5798
ITp	−0,12	0,2068
Central CT	−0,06	0,5540
ST	−0,08	0,4502
SN	−0,01	0,9337
IN	−0,03	0,7306
IT	−0,04	0,6514
STp	0,03	0,7675
SNp	−0,03	0,7302
INp	−0,004	0,9673
ITp	0,06	0,5115

(* Both r coefficients and p values were adjusted for the patients' age and gender.). RT: retinal thickness, CT: choroidal thickness, SN: superonasal, ST: superotemporal, IT: inferotemporal, IN: inferonasal, SNp: peripheral superonasal, STp: peripheral superotemporal, ITp: peripheral inferotemporal, INp: peripheral inferonasal.

Figure 2. Choroidal thickness in young (A) and older (B) individuals. A significant difference in the central CT is visible on the scans.
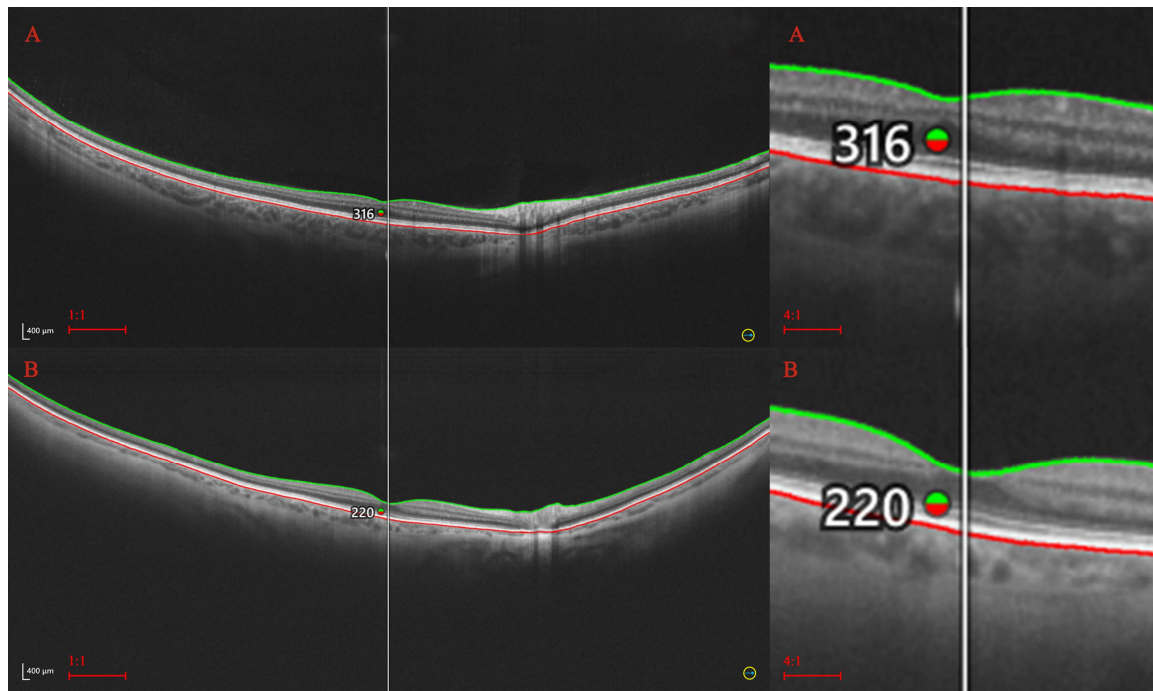
Figure 3. Retinal thickness in young (A) and older (B) individuals. A significant difference in the central RT is marked on the UWF-OCT scans.

4. Discussion

Most of the studies that analyzed retinal and choroidal thickness variation used traditional equipment with a standard field of view. Thus, most of the data refers to the area of the ETDRS grid with a maximum diameter of 6 mm, or a wider field of 12 mm width but rarely with the use of wide-field OCT scanning [10]. In our study, performed with wide-field equipment and 23 x 20 mm scans, we analyzed CT and RT values outside the central part of the posterior globe and provided additional data for those considerations. To our knowledge, this is the widest field of view available at present in OCT devices and as such, enables to draw more extensive picture of the architecture of the globe. Just a few other studies with the use of UWF-OCT, without the need for creating a mosaic of images, were performed so far [11,12]. In our study, the choroid has the shape of a convex-concave lens, with the peripheral thickness higher at the temporal side compared to the nasal side and the upper side compared to the inferior side. The retina has an approximately double convex shape with a thicker part located around the optic nerve. A similar picture of the retinal and choroidal architectures analyzed by the UWF testing was drawn by Hirano et [11]. In other studies such a difference between the architectures of these anatomical entities was also brought up , however in standard field OCT examination. For example Wang et al. analyzed variations in the central 6 mm circle (ETDRS grid) [13]. Rasheed et al. used a mosaic of OCT scans to obtain a wider field of view [14]. The authors noted a higher mean CT in vertical scans compared to horizontal ones and a smaller CT in all peripheral sectors, especially the inferior ones, which is consistent with our data.

Former studies on the variation of the CT in healthy individuals with the use of standard field OCT showed a similar percentage of symmetrical versus asymmetrical patterns and quite a high percentage of thick choroid in younger patients (subfoveal CT > 395 µm in 30% of cases younger than 55 years) [15]. This finding is confirmed by the results of our study: the third quartile value for the mean CT in the foveal area (3 mm in diameter) in patients younger than 40 is 395.50 µm, meaning that 25% in that age group have a higher CT.

One of the few WF-OCT studies, conducted by Kim et al., found symmetrical CT in both eyes in healthy individuals [12]. Nevertheless, differences in CT values between the eyes were greater at the periphery, indicating greater anatomical variations in the peripheral areas. In our study, the anatomical variation in thickness was similar for the central and peripheral areas.

4.1. Gender-Related Variations in RT and CT

In our study, men had generally greater retinal thickness compared to women, whereas women had significantly higher choroidal thickness compared to men. The CT in the central 3 mm part of the macula was similar in males and females, however, the peripheral sectors had significantly higher mean CT values in females. The use of UWF-OCT provides the possibility to show this difference , contrary to the standard field imaging. This topic has also been analyzed in other studies, although usually without WF-OCT. Wang et al. reported higher mean RT and CT values in men in an analysis that included only the central 6 mm circle corresponding to the ETDRS grid. On the other hand, a study by Zhang et al. with 12 x 9 mm scans did not report gender-related variations in RT and CT. A similar outcome was presented in Rasheed's study on healthy eyes, which involved a mosaic of OCT scans using Heidelberg Spectralis. It is plausible that, without including measurements of the choroidal periphery, such gender-related differences in CT and RT were not recorded. Our study suggests a greater volume of the whole choroid in females and a greater retinal volume in males.

4.2. Age-Related Variations in RT and CT

An important consideration is the relation of the retinal and choroidal thicknesses to the patient's age, especially considering that normal choroidal thickness values strongly impact analysis in the context of pachychoroid spectrum diseases. In our study, both CT and RT are generally strongly correlated with the patient's age; the exceptions are far peripheral retinal areas that do not show such a strong variation. The correlation is particularly apparent for the choroid, which significantly loses thickness over time in all sectors. Thus, CT evaluation in the pachychoroid spectrum must take into account choroidal thinning occurring in older age. This also concerns the peripheral choroid, whose thickness is also clearly dependent on the patient's age. This finding, maybe not surprising, but presents as novel in the context of available research that employed just a standard field OCT imaging.

Variations in the choroidal and retinal thicknesses with age were analyzed in a few studies. Similar results to ours were reported by Hirano et al. for UWF-OCT [11]. In a study of the ETDRS grid area, Pongsachareonnont et al. also found a significant loss of retinal and choroidal thickness with age; only the nerve fiber layer thickness was age-independent. Similar findings were reported for the choroid by Xie et al. and Cortes et al. in studies with standard field OCT [5,16]. The authors reported significant CT loss over the age of 50. Wang et al. also reported the loss of total RT and CT in older patients. Zhang noted lower CT values in older people using SS-OCT 12 x 9 mm scans [17]. Thinner peripapillary choroid in older individuals was also reported by Yang et al. [18]. The authors calculated a loss of 9 μm of total CT per decade. On the other hand, Rasheed et al. did not find CT variations with age. Such a lack of age dependence for RT and CT is seldom reported.

4.3. Axial Length and the RT and CT

Our study did not find a significant influence of the axial length on the measurement of RT and CT after adjusting for age and gender. This result refers also to the far periphery of the retina and choroid. The data on such correlations vary among studies. Mansoori et al., Yao et al., and Abbey et al. reported thinner central choroid and retina in longer eyeballs [19–21]. All these studies used standard field OCT scans. On the other hand, in a wide-field study, Hirano et al. found a weak negative correlation for selected sectors of the choroid. Nadeem did not find such a correlation in a large group of children [22]. Our analysis differs from most previous studies as it applied both multifactor statistic modeling (age and gender adjustment) and wide-field OCT testing. As such, and given the lack of large studies employing UWF-OCT, the present study should be treated as a stand-alone research and should not be simply compared with data from other papers.

4.4. CT and RT and Ocular Diseases

Retinal and choroidal thickness are strongly associated with occurrence of ocular diseases. That refers for both, straightforward situations , such as typical retinal edema, but also variations in retinal thickness in general, that can precede the disease onset, sustain a risk factor for its development or prognose its course. Such variations have been reported in such clinical entities as diabetic retinopathy or retinal vein occlusion [23–25]. Analysis of choroidal thickness led to identification of

spectrum of pachychoroid disorders, in which increased CT and congestion of choriocapillaris underly the mechanism of penetration of serous fluid under neurosensory retina [26,27]. Visualization and measurements of CT can also supply information on the state of ocular circulation or its deficit, what has a correlation with the onset of degenerative diseases such as retinal degenerations and dystrophies [28–30].   Providing CT measurements has potential for monitoring disease activity in the follow-up of inflammatory choroidal disorders or immunological choroidopathies as well as choroidal tumors or granulomas [31–33].

For all such analysis the normative database is necessary to serve as reference. Despite large variation of RT and CT according to age or gender, it is important to outline the possible ranges of that thicknesses that would constitute a benchmark . The wide field OCT systems are just introduced to clinical practice, so the information on far peripheral retinal and choroidal thickness is still a subject for analysis. The normative database for peripheral RT and CT can stand as a basis for the further research on involvement of these regions in ocular pathologies.

5. Conclusion

Ultra-wide field optical coherence tomography (UWF-OCT) scanning enables one to picture the shape of the retina and choroid in a large portion of the eyeball. In general, the UWF picture of the architecture of the globe confirms findings of standard field studies. Both anatomical entities get significantly thinner at the periphery and this trend is maintained preserved on the UWF-OCT at the far peripheral areas.. The peripheral choroid thickness (CT) is greater in the upper and temporal sectors. Both the choroid and retina lose thickness with age, however, the CT and retinal thickness (RT) do not show a statistically significant correlation with axial length after adjusting for age and gender. Age-related variations refer to both central and peripheral regions and are especially prominent for the choroid. The CT on UWF-OCT testing is significantly greater in females and the RT is greater in males.

References

1. Realini T, Zangwill LM, Flanagan JG, Garway-Heath D, Patella VM, Johnson CA, Artes PH, Gaddie IB, Fingeret M. Normative Databases for Imaging Instrumentation. J Glaucoma. 2015 Aug;24(6):480-3.
2. Nakayama, L.F., Zago Ribeiro, L., de Oliveira, J.A.E. *et al.* Fairness and generalizability of OCT normative databases: a comparative analysis. *Int J Retin Vitr* **9**, 48 (2023).
3. Palazon-Cabanes A, Palazon-Cabanes B, Rubio-Velazquez E, Lopez-Bernal MD, Garcia-Medina JJ, Villegas-Perez MP. Normative Database for All Retinal Layer Thicknesses Using SD-OCT Posterior Pole Algorithm and the Effects of Age, Gender and Axial Lenght. J Clin Med. 2020 Oct 15;9(10):3317.
4. Invernizzi A, Pellegrini M, Acquistapace A, Benatti E, Erba S, Cozzi M, Cigada M, Viola F, Gillies M, Staurenghi G. Normative Data for Retinal-Layer Thickness Maps Generated by Spectral-Domain OCT in a White Population. Ophthalmol Retina. 2018 Aug;2(8):808-815.e1.
5. Cortés DA, Roca D, Navarro PI, Rodríguez FJ. Macular and choroidal thicknesses in a healthy Hispanic population evaluated by high-definition spectral-domain optical coherence tomography (SD-OCT). Int J Retina Vitreous. 2020 Dec 7;6(1):66.
6. Entezari M, Karimi S, Ramezani A, Nikkhah H, Fekri Y, Kheiri B. Choroidal Thickness in Healthy Subjects. J Ophthalmic Vis Res. 2018 Jan-Mar;13(1):39-43.
7. Silva PS, Cavallerano JD, Haddad NM, Kwak H, Dyer KH, Omar AF, Shikari H, Aiello LM, Sun JK, Aiello LP. Peripheral Lesions Identified on Ultrawide Field Imaging Predict Increased Risk of Diabetic Retinopathy Progression over 4 Years. Ophthalmology. 2015 May;122(5):949-56..
8. Ashraf M, Cavallerano JD, Sun JK, Silva PS, Aiello LP. Ultrawide Field Imaging in Diabetic Retinopathy: Exploring the Role of Quantitative Metrics. J Clin Med. 2021 Jul 27;10(15):3300.
9. Orski M, Gawęcki M. Current Management Options in Irvine-Gass Syndrome: A Systemized Review. J Clin Med. 2021 Sep 25;10(19):4375.
10. Pongsachareonnont P, Somkijrungroj T, Assavapongpaiboon B, Chitamara T, Chuntarapas M, Suwajanakorn D. Foveal and parafoveal choroidal thickness pattern measuring by swept source optical coherence tomography. Eye (Lond). 2019 Sep;33(9):1443-1451.
11. Hirano M, Muraoka Y, Kogo T, Ishikura M, Nishigori N, Ueda-Arakawa N, Miyata M, Hata M, Takahashi A, Miyake M, Tsujikawa A. Analysis of widefield choroidal thickness maps of healthy eyes using swept source optical coherence tomography. Sci Rep. 2023 Jul 24;13(1):11904.

12. Kim MS, Lim HB, Lee WH, Kim KM, Nam KY, Kim JY. Wide-Field Swept-Source Optical Coherence Tomography Analysis of Interocular Symmetry of Choroidal Thickness in Healthy Young Individuals. Invest Ophthalmol Vis Sci. 2021 Mar 1;62(3):5.

13. Wang J, Gao X, Huang W, Wang W, Chen S, Du S, Li X, Zhang X. Swept-source optical coherence tomography imaging of macular retinal and choroidal structures in healthy eyes. BMC Ophthalmol. 2015 Sep 17;15:122.

14. Rasheed MA, Singh SR, Invernizzi A, Cagini C, Goud A, Sahoo NK, Cozzi M, Lupidi M, Chhablani J. Wide-field choroidal thickness profile in healthy eyes. Sci Rep. 2018 Nov 21;8(1):17166.

15. Touhami S, Philippakis E, Mrejen S, Couturier A, Casteran C, Levent P, Tadayoni R, Gaudric A. Topographic Variations of Choroidal Thickness in Healthy Eyes on Swept-Source Optical Coherence Tomography. Invest Ophthalmol Vis Sci. 2020 Mar 9;61(3):38.

16. Xie J, Ye L, Chen Q, Shi Y, Hu G, Yin Y, Zou H, Zhu J, Fan Y, He J, Xu X. Choroidal Thickness and Its Association With Age, Axial Length, and Refractive Error in Chinese Adults. Invest Ophthalmol Vis Sci. 2022 Feb 1;63(2):34.

17. Zhang C, Tatham AJ, Medeiros FA, Zangwill LM, Yang Z, Weinreb RN. Assessment of choroidal thickness in healthy and glaucomatous eyes using swept source optical coherence tomography. PLoS One. 2014 Oct 8;9(10):e109683.

18. Yang H, Luo H, Gardiner SK, Hardin C, Sharpe GP, Caprioli J, Demirel S, Girkin CA, Liebmann JM, Mardin CY, Quigley HA, Scheuerle AF, Fortune B, Chauhan BC, Burgoyne CF. Factors Influencing Optical Coherence Tomography Peripapillary Choroidal Thickness: A Multicenter Study. Invest Ophthalmol Vis Sci. 2019 Feb 1;60(2):795-806.

19. Mansoori T, Charan ASR, Nagalla B. Topography and Choroidal Thickness Measurement in Healthy Asian Indian Subjects using RTVue XR 100 Optical Coherence Tomography. Middle East Afr J Ophthalmol. 2024 Jan 22;30(1):19-23.

20. Yao Y, Fu J, Liu J, Li L, Chen W, Meng Z. Assessment of macular choroidal and retinal thickness: a cohort study in Tibetan healthy children. Sci Rep. 2024 Jan 16;14(1):1383.

21. Abbey AM, Kuriyan AE, Modi YS, Thorell MR, Nunes RP, Goldhardt R, Yehoshua Z, Gregori G, Feuer W, Rosenfeld PJ. Optical coherence tomography measurements of choroidal thickness in healthy eyes: correlation with age and axial length. Ophthalmic Surg Lasers Imaging Retina. 2015 Jan;46(1):18-24.

22. Nadeem S. Macular choroidal thickness and correlations in a healthy pediatric South Asian cohort: A spectral domain optical coherence tomography study. J Biophotonics. 2023 Jul;16(7):e202300039.

23. Jiang J, Liu Y, Chen Y, Ma B, Qian Y, Zhang Z, Zhu D, Wang Z, Xu X. Analysis of Changes in Retinal Thickness in Type 2 Diabetes without Diabetic Retinopathy. J Diabetes Res. 2018 Feb 25;2018:3082893.

24. Boned-Murillo, A.; Fernández-Espinosa, G.; Orduna-Hospital, E.; Díaz-Barreda, M.D.; Sánchez-Cano, A.; Sopeña-Pinilla, M.; Bielsa-Alonso, S.; Pinilla, I. Changes in Inner Retina Thickness and Macular Sensitivity in Patients with Type 2 Diabetes with Moderate Diabetic Retinopathy. *Biomedicines* **2023**, *11*, 2972.

25. Yin S, Cui Y, Jiao W, Zhao B. Potential Prognostic Indicators for Patients With Retinal Vein Occlusion. Front Med (Lausanne). 2022 May 25;9:839082.

26. Hua R, Duan J, Zhang M. Pachychoroid Spectrum Disease: Underlying Pathology, Classification, and Phenotypes. Curr Eye Res. 2021 Oct;46(10):1437-1448.

27. Safi H, Ahmadieh H, Hassanpour K, Safi S. Multimodal imaging in pachychoroid spectrum. Surv Ophthalmol. 2022 Mar-Apr;67(2):579-590.

28. Baek J, Lee JH, Jung BJ, Kook L, Lee WK. Morphologic features of large choroidal vessel layer: age-related macular degeneration, polypoidal choroidal vasculopathy, and central serous chorioretinopathy. Graefes Arch Clin Exp Ophthalmol. 2018 Dec;256(12):2309-2317.

29. Sabbaghi H, Ahmadieh H, Jalili J, Behnaz N, Fakhri M, Suri F, Kheiri B, Rajabpour M, Entezari M, Daftarian N. Choroidal Thickness in Different Types of Inherited Retinal Dystrophies. J Ophthalmic Vis Res. 2020 Aug 6;15(3):351-361.

30. Abdolrahimzadeh S, Di Pippo M, Ciancimino C, Di Staso F, Lotery AJ. Choroidal vascularity index and choroidal thickness: potential biomarkers in retinitis pigmentosa. Eye (Lond). 2023 Jun;37(9):1766-1773.

31. Baltmr A, Lightman S, Tomkins-Netzer O. Examining the choroid in ocular inflammation: a focus on enhanced depth imaging. J Ophthalmol. 2014;2014:459136.

32. Dalvin LA, Shields CL, Ancona-Lezama DA, Yu MD, Di Nicola M, Williams BK Jr, Lucio-Alvarez JA, Ang SM, Maloney SM, Welch RJ, Shields JA. Combination of multimodal imaging features predictive of choroidal nevus transformation into melanoma. Br J Ophthalmol. 2019 Oct;103(10):1441-1447.

33. Agarwal A, Aggarwal K, Pichi F, Meng T, Munk MR, Bazgain K, Bansal R, Agrawal R, Gupta V. Clinical and Multimodal Imaging Clues in Differentiating Between Tuberculomas and Sarcoid Choroidal Granulomas. Am J Ophthalmol. 2021 Jun;226:42-55.

disclaim responsibility for any injury to people or property resulting from any ideas, methods, instructions or products referred to in the content.